J. Membrane Biol. 154, 143–153 (1996)

The Journal of
Membrane
Biology

Characterization of a Neuronal Delayed Rectifier K Current Permeant to Cs and Blocked by Verapamil

C. Trequattrini, A. Petris, F. Franciolini
Dipartimento Biologia Cellulare e Molecolare, Università di Perugia, Via Pascoli 1, 06100 Perugia, Italy

Received: 12 May 1996/Revised: 19 July 1996

Abstract. We have used the patch-clamp method in the whole-cell configuration to characterize the delayed rectifier K current (I_{DRK}) in embryonic chick dorsal root ganglion (DRG) neurons. The I_{DRK} is activated by depolarizing pulses positive to −40 mV, and its $V_{1/2}$ is near −20 mV. The slope factor of 10.4 mV for an e-fold change in conductance indicates an equivalent gating charge of 2.4e. Inactivation during sustained depolarizing pulses displays two distinct time constants of 200–300 msec and 6–9 sec, respectively. Outward current through the delayed rectifier K (DRK) channels could also be carried by internal Cs, which however exerts mild block when in mixtures with K, as evidenced by the anomalous mole fraction effect. The relative permeability of Cs *vs.* K, P_{Cs}/P_K, as calculated from reversal potential measurements, is 0.25. Rb likewise permeates the DRK channel ($P_{Rb}/P_K = 0.67$). The I_{DRK} was effectively suppressed by external application of the Ca channel blocker Verapamil, with apparent dissociation constant of *ca.* 4 μM. The time course of Verapamil block, its good description by equations derived from open-channel block kinetic scheme, and the frequency-dependent effect of the blocker indicate that Verapamil can bind to the channel only when it is in the open state.

Key words: DRG neurons — Ion channels — K currents — Patch clamp — Embryonic neurons — K channel selectivity — Verapamil

Introduction

I_{DRK} have been extensively characterized in many excitable membranes, and found to share several basic properties. In briefly reviewing past work, the current activates upon depolarizing pulses to voltages more positive than −40 mV, and generally inactivates slowly during sustained depolarization (Ehrenstein & Gilbert, 1966; Schwarz & Vogel, 1971). Inactivation usually follows mono- or multi-exponential relaxation with the slowest time constant normally greater than several hundred msec (Schwarz & Vogel, 1971). DRK channels select poorly among K, Rb, and Tl which can readily permeate the channel and carry appreciable current (Binstock & Lecar, 1969; Bezanilla & Armstrong, 1972; Hille, 1973). The other alkali cations Li, Na, and Cs not only are impermeant, but block the DRK channel when applied intracellularly, with Cs being the most powerful of the three (French & Wells, 1977; Adelman & French, 1978; Bezanilla & Armstrong, 1972). Cs in addition can block inward K currents also when applied extracellularly (Adelman & French, 1978). The only relevant exception to this pattern is represented by snail neurons where P_{Cs}/P_K was found equal to 0.18 (Reuter & Stevens, 1980).

Studying the K currents of embryonic chick DRG neurons, we found that the I_{DRK} in this preparation differs from most DRK channels for passing Cs, which was capable of sustaining considerable current. In addition, we found that the I_{DRK} was blocked by micromolar concentrations of Verapamil, a typical Ca channel blocker, recently reported to block K channels, in a state-dependent manner, from several tissues (Pancrazio et al., 1991; Rampe et al., 1993; DeCoursey, 1995). These features, combined with the poor characterization of the I_{DRK} in this preparation (*cf.* Nowycky, 1992), prompted up to extend the study of this current with two general objectives. To investigate the general form of I_{DRK}, and the interaction of Cs ions and the drug Verapamil with the DRK channel.

Materials and Methods

Whole-cell currents were recorded from DRG neurons dissociated from 9–11-day-old chick embryos (Barde, Edgard & Thoenen, 1980). Gan-

Correspondence to: F. Franciolini

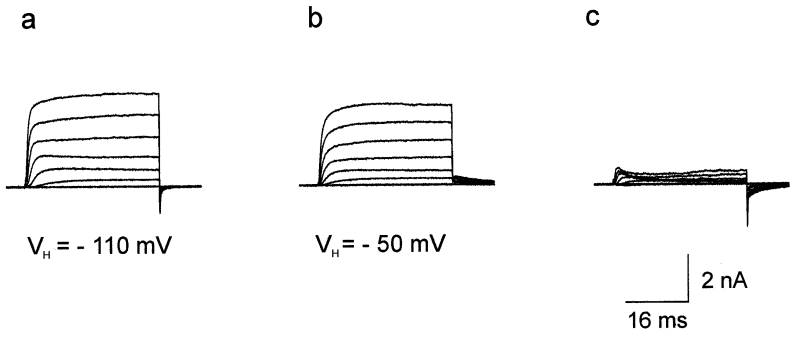

Fig. 1. Effects of voltage manipulation on outward K currents. (*a*) Current traces elicited by depolarizing pulses from −60 to +60 mV in 20 mV increments (V_H = −110 mV). (*b*) Same pulse protocol as in *a*, but from V_H = −50 mV. (*c*) Difference between records in *a* and *b*. Bath solution contained 140 NaCl, as main salt.

glia were dissociated into single cells by gentle compression through pipettes with increasingly smaller tip diameters. Dissociated cells were plated in Petri dishes coated with poly-D-lysine, and used for the experiments 2–8 hr after plating. The whole-cell configuration of the patch-clamp method (Hamill et al., 1981) was used with borosilicate pipettes whose resistance ranged between 1 and 2 MΩ when filled with standard pipette solutions. In these conditions, access resistance to the cells of 4–6 MΩ were usually obtained. Normally, 60–80% of the series resistance was electronically compensated. The pClamp (Axon Instruments, Foster City, CA) package of hardware and software was routinely used for stimulating the command voltage, recording the currents, and preliminary analysis of the data. Curve fitting was usually performed with SigmaPlot, or with the q-matrix method (Colquhoun & Hawkes, 1977) when, due to the complexity of the kinetic scheme, a symbolic equation could not be derived. We developed a program that incorporated the q-matrix method into an optimization routine to determine kinetic rate constants best describing the macroscopic currents. For online data collection, current signals were usually filtered at 5–10 kHz and digitized at 20–100 kHz. Capacitive transients and series resistance were mostly compensated electronically. Linear leakage currents and residual capacitive transients were eliminated by using P/4 stimulation protocols. All the experiments were carried out at room temperature (18–22°C). Except where differently specified, the pipette solution contained (in mM): 145 KCl, 1 $CaCl_2$, 2 $MgCl_2$, 11 EGTA, 2 MOPS buffer at pH 7.3. In some experiments 140 CsCl was used in place of KCl. In these conditions, the estimated intracellular Ca concentration is lower than 10 nM. The bath solution usually contained (in mM): 140 NaCl, 5 $CaCl_2$, 2 $MgCl_2$, 0.5 Cd, $0.5 \cdot 10^{-3}$ TTX and 2 MOPS buffer at pH 7.2. In selectivity experiments, 140 NaCl was replaced by equimolar concentration of the test ion.

In the experiments where tail current measurements were necessary, 140 NaCl was replaced by 140 KCl. Verapamil was daily dissolved at the final concentration in the same solution and superfused on the cell. For the selectivity experiments, NaCl was replaced by the same concentration of a chloride salt of the test cation. Solutions bathing the cells were changed by manually lowering a large bore pipette that contained the desired test solution near the cell. Junction potentials of these solutions were measured for each solution (with respect to a reference electrode: 476012, Corning Medical, Medfield, MA), and used to correct the applied voltage steps in the selectivity experiments. Data are expressed as mean ± SEM.

Results

Isolation of I_{DRK}

Outward K currents usually result from a combination of Ca-activated and voltage-dependent K currents. A contribution of Ca-activated K current to the outward K current could be excluded in our experimental conditions given the external presence of the Ca channel blocker Cd that prevents Ca influx, and intracellular presence of 11 mM EGTA. The voltage-dependent outward K current in most neuronal preparations is comprised of two major components that differ in kinetics and steady-state inactivation: the delayed rectifier, and the fast transient K current (Connor & Stevens, 1971; Neher, 1971; Hermann & Gorman, 1981; Kostyuk et al., 1981; Belluzzi, Sacchi & Wanke, 1985). The fast transient K current, I_A, activates and inactivates at membrane potentials ca. 30 mV negative to the corresponding potentials for the I_{DRK}. This difference in voltage domain has been successfully used in many instances to dissect these two currents. In particular, since I_A is generally inactivated completely at V_H as positive as −50 mV, a voltage at which the I_{DRK} is almost entirely available, conditioning the cell at this voltage is usually an effective method.

We used this protocol on embryonic chick DRG neurons, and found it effective in eliminating the I_A component, which is however negligible in this preparation. This is illustrated in Fig. 1 (representative of five experiments) which shows two families of K currents activated by depolarizing pulses from −60 to +60 mV, from two different conditioning voltages of −110 and −50 mV (Fig. 1*a* and *b*), together with the difference between the current traces at these two conditioning voltages, which should represent the I_A component. The resulting transient component shown in Fig. 1*c* is clearly negligible. The steady-state component that remains after the subtraction procedure is due to partial steady-state inactivation of the I_{DRK} that occurs at V_H = −50 mV. The marginal presence of the I_A component in DRG neurons was confirmed by experiments (*not shown*) using the I_A blocker 4-AP, a compound widely used for separating different components of outward *K* currents in neurons. In these experiments (n = 3), the amount of transient current suppressed by application of 1 mM of 4-AP was similar to that eliminated by voltage manipulation.

Although both methods indicate that the I_A component in this preparation is negligible, we have studied the I_{DRK} by conditioning the cells to a V_H = −70 mV, as a

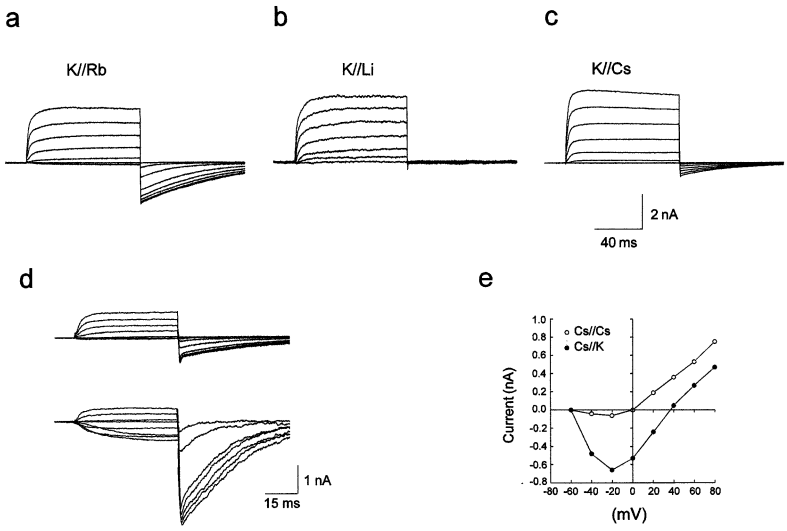

Fig. 2. Selectivity of the DRK channel. Upper panels, current traces from three different cells, with different ions in the bath (indicated), and 150 KCl in the pipette. All currents were activated by 100 msec pulses to potentials varying from −60 to +60 mV in 20 mV increments. $V_H = -70$ mV. Lower panels, selectivity test for Cs through DRK channels. (*d*) Families of current were recorded in symmetrical 150 Cs solution (upper traces), and after replacement of bath solution with 150 KCl (lower traces). Currents were activated by 50 msec pulses to potentials varying between −60 to +80 mV, from $V_H = -70$ mV. (*e*) *I/V* plot of current traces shown in (*d*). Reversal potential was shifted from 0 mV of the symmetrical CsCl conditions, to +37 mV upon replacement of external 150 CsCl with 150 KCl.

compromise between I_{DRK} preservation and I_A suppression. 4-AP was not used because at the concentration (millimolar) necessary to block I_A it affects several features of the I_{DRK}. Namely, it reduces the voltage-dependence of I_{DRK} (less reduction at more positive voltages), and slows its onset rate (Pelhate & Pichon, 1974; Yeh et al., 1976; Shauf et al., 1976; Ulbricht & Wagoner, 1976; Meves & Pichon, 1977; Hermann & Gorman, 1981). Other ionic pathways were eliminated by using specific channel blockers, or large impermeant ion replacements (*cf.* Materials and Methods).

Selectivity

In addition to showing the efficacy of the method for isolating the I_{DRK}, the absence of tail currents in Fig. 1 also shows that Na cannot permeate these channels. To test whether other alkali cations were permeant we superfused the cell in turn with Li, Rb, and Cs. The results presented in Fig. 2*a–c* show that tail currents upon repolarization to −80 mV, indicating an influx of external cations through the DRK channel (the only functional channel present), were observed with Rb and Cs, but not with Li. The permeant ions Rb and Cs were also found to sustain outward currents when the cell was internally perfused with either one of these ions (*see* Fig. 2*d* for Cs). The permeability ratio between the two permeant alkali ions, Rb and Cs, *vs.* K was assessed from reversal potential (E_{rev}) measurements. For a more precise evaluation of E_{rev} shifts, and taking advantage of the ability of Rb and Cs to sustain outward currents, we carried out experiments which would start with symmetrical conditions of the Cl salt of the test ion Rb or Cs (to which a $E_{rev} = 0$ mV corresponds), followed by replacement of the external solution with KCl. In these conditions, E_{rev} shifts in the positive direction of 26 ± 3 ($n = 7$) and 37 ± 5 ($n = 3$) mV were obtained respectively for Rb and Cs. These shifts can be accounted for in the Goldman-Hodgkin-Huxley voltage equation by permeability ratios $P_{Rb}/P_K = 0.67$ and $P_{Cs}/P_K = 0.25$. Since, contrary to Rb, Cs has been generally found only negligibly permeable through the DRK channel, for this ion a representative experiment to quantitate the permeability of this ion with respect to K is shown (Fig. 2*d–e*). We also measured the conductance ratio between Cs and K by averaging the outward current amplitude (weighted for the cell capacitance) obtained with cells perfused with internal Cs ($n = 14$) and internal K ($n = 49$). The calculated value of g_{Cs}/g_K was 0.18.

As Cs is both permeant and weakly conducting, we tested for Cs block of the current through DRK channels by running the anomalous mole-fraction experiment. We measured the inward (tail) current amplitudes produced by Cs and K present externally either singly, or as a mixture, always at a total external concentration of 70 mM (osmolarity was adjusted by adding 70 mM choline chloride). We chose to measure the inward current since this allowed the replacement of the (external) solution, and thus the current measurements in pure Cs, in pure K, and in a mixture of the two ions on the same cell. Figure 3*a* illustrates a representative experiment consisting of three superimposed current traces recorded in solutions containing Cs and K at varying proportions (indicated). Figure 3*b* plots the fractional tail current from eight cells as function of the molar fraction of Cs in the external solution. The plot clearly shows that there is no linear dependence between current amplitude and Cs concentration. In particular, in the presence of Cs, the amplitude of the current is smaller than that expected if K and Cs fluxes through the channel were independent.

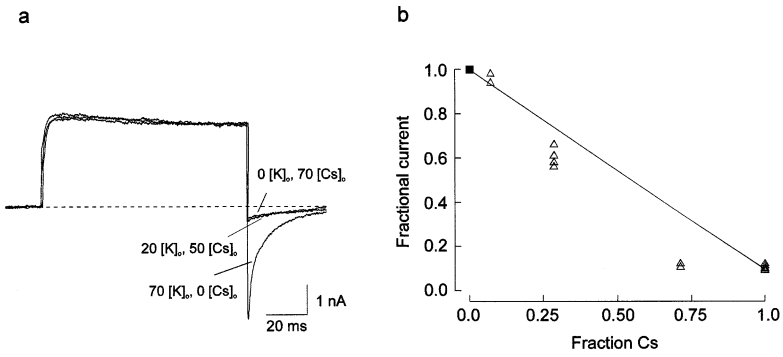

Fig. 3. Anomalous mole fraction effect. (*a*) Superimposed membrane currents in response to same depolarizing step at +40 mV, followed by repolarization to −80 mV (V_H = −70 mV), in different mixtures of K and Cs (indicated). For accurate measurements, tail currents were exponentially fit, and the zero amplitude point was taken as I_{tail}. (*b*) Fractional tail current as function of mole-fraction of Cs in the external solution.

Verapamil Block

A very effective blocker of the I_{DRK} in this preparation was found to be Verapamil, a representative of the phenylalkylamine Ca channel blocker family. In Fig. 4*a*, the effects of external application of 30 μM of Verapamil on the I_{DRK} evoked by a depolarizing pulse at +100 mV are shown. In the presence of Verapamil, current traces exhibited an initial peak, followed by a fast decay to a steady-state value. Both the reduction in peak current amplitude and the residual steady-state value were a function of Verapamil concentration. The activation rate of the current was by contrast unaffected by the drug. Such kinetics of blocking are consistent with a mechanism first described by Armstrong (1971) for I_{DRK} blocking in the squid giant axon by quaternary ammonium ions, where the blocker can bind to the channel only when it is in the open state. The applicability of this mechanism of blocking to our results is indicated by the good fit of the current traces in presence of Verapamil (superimposed in Fig. 4*a*) that could be obtained with the equation resulting from the open-channel block kinetic scheme (*see* legend to Fig. 4 for details). Further evidence that Verapamil blocks in a state-dependent manner is provided by a use-dependent effect shown by the drug (Fig. 4*c*). A 5-Hz train of 25 msec-depolarizing pulses from a V_H of −70 to +60 mV was applied to a cell in control conditions and after application of 30 μM of Verapamil. In the absence of Verapamil, there was no reduction of I_{DRK} with successive pulses, whereas a substantial use-dependent reduction of I_{DRK} was observed after addition of the drug. Figure 4*c* shows current traces obtained with the above stimulation protocol. Maximal current amplitudes (I_{max}) were then plotted as function of pulse number, for control (circles) and Verapamil (squares) in Fig. 4*d*.

A quantitative analysis of the blocking effect of Verapamil on I_{DRK} was carried out by constructing a dose-response curve. I_{DRK} were elicited by depolarizing pulses at +100 mV in the presence of different concentrations of Verapamil. The residual steady-state current, expressed as percent of I_{max} in control conditions, was plotted against Verapamil concentration. Data were well fit by a single-site absorption isotherm (Fig. 4*b*) of the form given in the figure legend. The curve fit gave an apparent K_D of 3.9 μM. Verapamil was also found to block Cs outward currents through DRK channels with similar time course and efficacy as observed with K (*data not shown*). A detailed study of the Verapamil block of I_{DRK} on this preparation is under way.

The Sustained Outward Current Does Not Pass through Ca Channels

Data presented so far describe a noninactivating, voltage-dependent, poorly selective K channel not significantly blocked by the classical DRK channel blocker Cs, but blocked by the Ca channel antagonist Verapamil. Similar noninactivating, nonselective outward currents sustained by alkali cations have been observed under certain experimental conditions in several preparations and interpreted as cationic currents through Ca channels (Kostyuk & Krishtal, 1977; Reuter & Sholtz, 1977; Lee & Tsien, 1982; Almers, McCleskey & Palade, 1984; Almers & McCleskey, 1984; Fukushima & Hagiwara, 1985). This occurrence introduces uncertainties with respect to the actual channel type sustaining the outward Cs current reported here. Uncertainties that remain even when external Cd is used to block Ca channels, since Cd may be ineffective at large depolarizations. This question is now addressed.

In the presence of both the sustained outward Cs current and the inward Ca current (which can be made visible by omitting the Ca channel blocker Cd from the extracellular medium (*cf.* Fig. 5)), functional elimination of Ca channels completely suppresses the inward Ca current, while leaving the outward Cs current virtually unaltered. One method used to obtain this result is through rundown, a time-dependent process that functionally eliminates Ca channels (Byerly & Hagiwara, 1982; Fenwick, Marty & Neher, 1982). In our experiments (n =

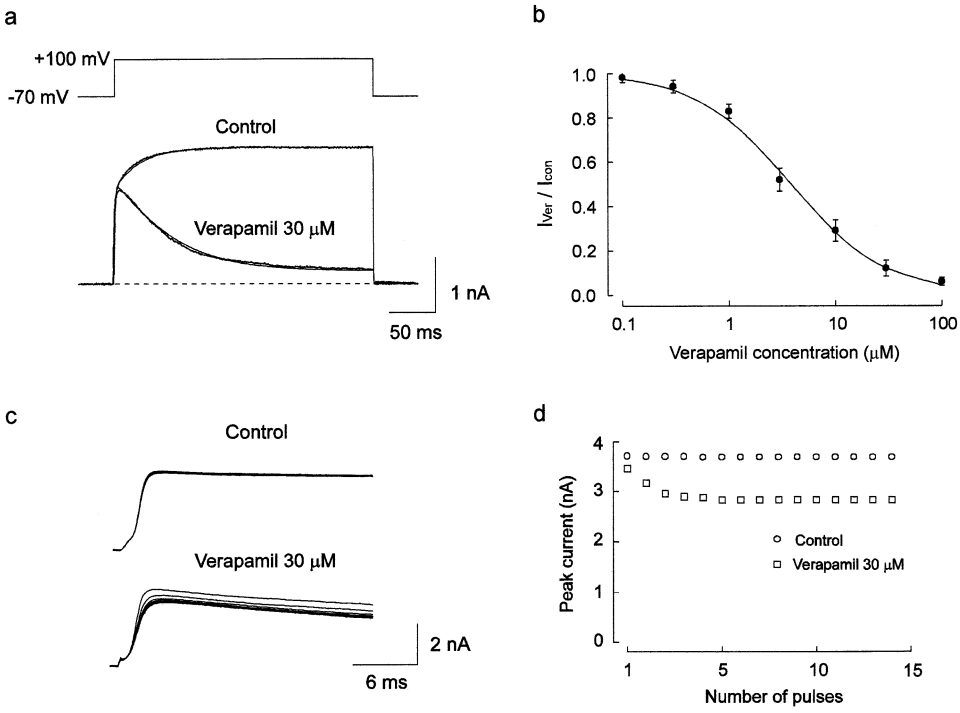

Fig. 4. State-dependent block of I_{DRK} by external Verapamil. (*a*) I_{DRK} evoked by a depolarizing pulse to +100 mV (V_H = −70), in control conditions, and after addition of 30 μM of Verapamil. Curve fitting (superimposed) was done with equations obtained by the q-matrix method (Colquohun & Hawkes, 1977; *see also* Materials and Methods). A satisfactory fit of the control trace that would account for the slow upward creep of the current could be obtained by using the kinetic scheme $C_1 \Leftrightarrow C_2 \Leftrightarrow O$ (C = closed states and O = open state; Koumi et al., 1994; also *cf.* Keynes et al., 1988), and letting the computer choose freely the initial occupancy of the closed states and rate constants. The trace with Verapamil was fit by using the minimal open-channel block kinetic scheme $C_1 \Leftrightarrow C_2 \Leftrightarrow O \Leftrightarrow O \cdot B$ ($O \cdot B$ = open-blocked state) with opening and closing rate constants as obtained from the fit of the control current trace. Best fit of the trace gave for block and unblock rate constants the values of 1.3 $msec^{-1}$ mM^{-1} and 0.004 $msec^{-1}$ respectively. (*b*) Dose-response curve for Verapamil obtained from 3–5 neurons. Data are expressed as fractional current (±SEM) at steady-state, with respect to control *vs.* drug concentration. Data points fit with a single-site absorption isotherm of the form $I_{Ver}/I_{con} = 1/(1 + [V]/K_D)$ gives an apparent K_D of 3.9 μM. (*c*) I_{DRK} in control (upper traces) and in 30 μM Verapamil (lower traces) evoked by 25 msec depolarizing pulses to +60 mV (V_H = −70), at a frequency of 5 Hz. (*d*) Plot of peak current amplitudes from the traces in *c* as function of pulse number.

4), rundown progressively eliminated inward Ca currents, without significantly affecting the sustained outward currents. One of these is illustrated in Fig. 5*a–c*, and shows three families of curves recorded at different times, in conditions of symmetrical 140 CsCl, and 5 Ca in the bath. Control traces show both the inward Ca and the sustained outward Cs components of comparable size. Records at later times (namely, 5 and 9 min after establishing the whole-cell configuration) manifest a progressive decrease and final suppression of the inward Ca current, while the noninactivating outward Cs component is only slightly affected. The disappearance of the inward Ca current as result of functional elimination of Ca channels due to rundown, and the persistence of the sustained outward component indicate that the inward and the outward currents are associated with different channels, one eliminated by rundown, the other resistant to it. The small residual current that can be observed in Fig. 5*c* is most probably the result of inward K through DRK channels (*cf.* Fig. 1*c*).

Measurements of reversal potential provide additional evidence that the two current components have distinct permeation pathways. A cell in which inward and outward currents pass through the same channel must show a true reversal potential, i.e., a potential that remains constant provided that the ionic conditions (and temperature) are not modified. Maneuvers that increase or decrease the currents (for instance, application of agonists, blockers, potential prepulses), but do not change the ionic concentrations should have no effect on the reversal potential. This must hold true also when the currents decrease with time as a result of rundown. To assess the behavior of reversal potential in the rundown experiment, the *I/V* plot was constructed (Fig. 5*d*) which clearly shows that the reversal potential is not constant but shifted with time towards more negative voltages. Several other tests have been carried out in this respect,

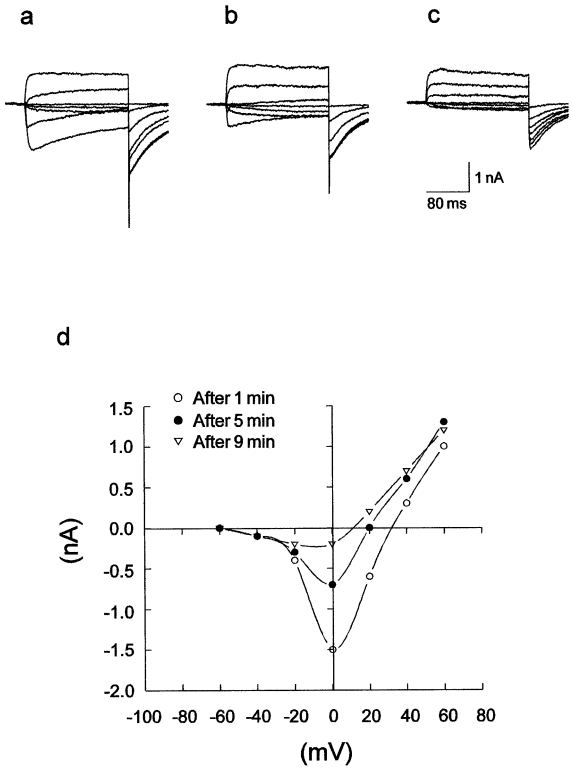

Fig. 5. Effect of rundown on inward and outward currents. The families of current were evoked by 200 msec depolarizing pulses ranging between −60 to +60 mV from V_H = −70 mV. Perfusion conditions were 150 CsCl//140 CsCl + 5 Ca; no Ca channel blocker present. (*a*) Control traces recorded 1 min after establishing whole-cell configuration. (*b*) and (*c*) After 4 and 8 min, respectively, from control recordings. (*d*) *I/V* plot of the peak current in *a* (open circles), *b* (filled circles), and *c* (open triangles), against time. As result of selective inhibition of inward current, reversal potential shifted from 33 to 20 mV (after 4 min), and to 10 mV (after 8 min).

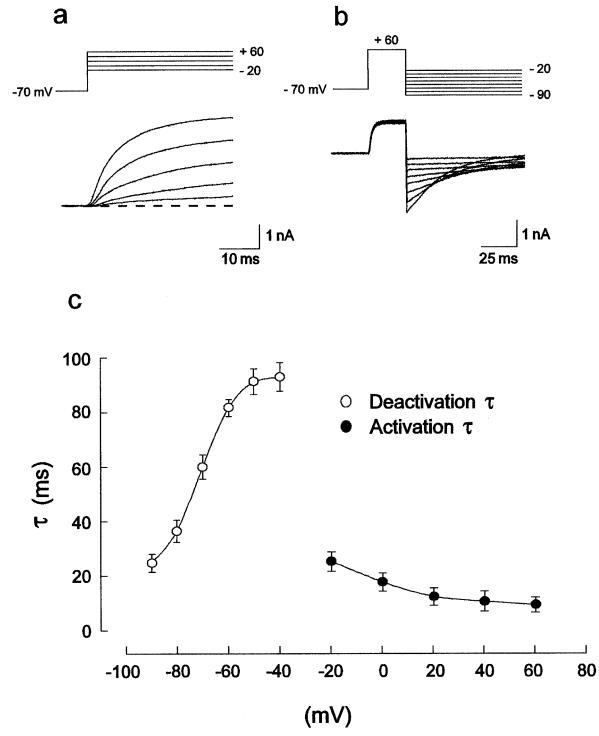

Fig. 6. Time constants for I_{DRK} activation and deactivation as function of voltage. (*a*) Family of I_{DRK} recorded during 40 msec depolarizing pulses from V_H = −70 mV to potentials ranging from −20 to +60 mV (20 mV steps). (*b*) Tail currents in response to repolarizing voltages from −90 to −20 mV (10 mV steps) after a constant depolarizing pulse of 25 msec at +60 mV. (*c*) Activation time constants (filled circles; n = 4) obtained from single-exponential fits done as described in the text. Deactivation (channel closing) time constants (empty circles; n = 4) obtained from single-exponential fits of tail currents. At potentials more positive than −40 mV, tail currents could not be fit reliably, and thus were not included in the plot.

which confirm the conclusions drawn from the rundown experiment.

Activation and Deactivation Kinetics

At all potentials I_{DRK} activates along a sigmoidal time course, with an initial lag period that depended on V_H. Activation curves representative of four experiments at different potentials are shown in Fig. 6*a*. We attempted to fit these current traces with the equation $I_t = I_{max} \cdot [1 - e^{-t/\tau}]^n$, where n was initially set equal to 4 in consideration of the four subunit composition of K channels (MacKinnon, 1991), and thus the assumed four voltage sensors present in the channel (*cf.* Catterall, 1988). The initial part of the current traces however could not be satisfactorily fit with n = 4 as well as with other values of n. We thus excluded the early delay interval from the fit and only fit the fast-rising phase of the activating current with a single exponential (although often a double-exponential would better account for the slow upward creep of the current following the initial fast-rising phase; *cf.* Fig. 4*a*, control trace) to obtain the main time constant of activation (White & Bezanilla, 1985; Spires & Begenisich, 1989), and facilitate comparison with other studies. The activation time constants of these single exponentials, plotted as a function of voltage in Fig. 6*c* (filled circles), were found to decrease with depolarization from *ca.* 25 msec at −20 mV to *ca.* 10 msec at +60 mV.

Deactivation time course of I_{DRK} shows a slow turn-off rate of the open channels. We quantified the deactivation kinetics by fitting the tail currents upon repolarization to varying potentials (from −90 to −20 mV) after fixed depolarizing pulse at +60 mV. A family of deactivating currents representative of four experiments is shown in Fig. 6*b*. Single exponentials resulted in a good fit of these currents for potentials more negative then −40 mV. The deactivation time constants were plotted as a function of voltage in Fig. 6*c* (open circles). Data at −30 and −20 mV were not included in the plot because at these potentials tail currents were difficult to fit reliably.

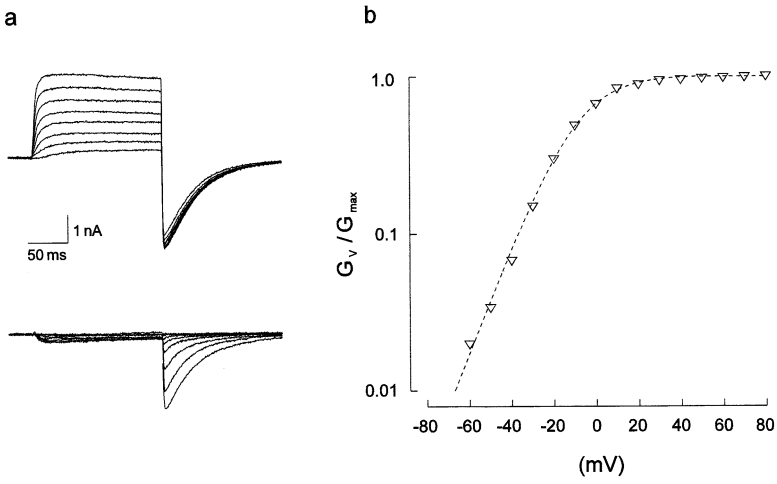

Fig. 7. Steady-state activation kinetics of I_{DRK}. (*a*) Family of currents evoked by depolarizing pulses from −60 to +80 mV (steps of 10 mV; V_H = −70 mV), with a constant post-pulse to −80 mV to obtain tail currents from which measurements were taken. The family of currents has been divided into two groups (upper and lower panels) for clarity. (*b*) Voltage dependence of steady-state I_{DRK} activation. The experimental points were fit by a Boltzmann function of the form $G_V/G_{max} = 1/(1 + e^{(V_{1/2}-V)/K})$, where G_{max} is the maximum conductance, G_V the conductance at the given voltage V, $V_{1/2}$ the voltage at which the conductance is half activated, and K is the slope factor describing the steepness of the activation curve. For this representative neuron, $V_{1/2}$ was equal to −17 mV and the slope factor K was 12 mV per e-fold change of G_V. In the case of a two-state gating particle gating the channel, as the good fit of the data with a Boltzmann distribution would suggest, the slope factor K describing the activation can be represented (Belluzzi et al., 1985) $K = kT/ze$, where k is the Boltzmann constant, T the absolute temperature, z the effective valency of the gating particle controlling the closed-open transition (the kinetics of activation), and e the elementary charge. In this case, the Boltzmann slope factor 12 gives an estimated minimum effective valency for gating of 2.1*e*.

Deactivation time constants were strongly voltage dependent increasing monotonically from *ca.* 25 msec at −90 mV to *ca.* 95 msec at −40 mV. The significant information from this figure is the much larger values of deactivation as compared to activation time constants that result in a discontinuous function of activation and deactivation τs *vs.* voltage.

A further descriptor of the activation kinetics of an ionic current is the steady-state conductance *vs.* voltage relationship. Conductances (normalized to maximal conductance) were obtained from deactivation tail current measurements at a fixed voltage of −80 mV, following depolarizing test pulses to various potentials from +80 to −60 mV (Fig. 7*a*). The normalized conductance values from experiments in separate neurons were then plotted on a logarithmic coordinate against the test membrane potential (Fig. 7*b*). The (averaged) experimental points were well fit by a single Boltzmann distribution with a slope factor of 10.4 ± 0.98 for an e-fold change in conductance (indicating an equivalent gating charge of 2.4e to open a single channel), and a $V_{1/2}$ of −19 ± 2.3 mV.

Inactivation

Because of the short recordings shown so far, the I_{DRK} time course may appear to be the result of a gating mechanism virtually lacking an inactivation process. A slow inactivation, however, develops and can be seen with long depolarizations of several seconds, as shown in Fig. 8*a*. Even with these long pulses inactivation is not complete. A percentage of current ranging between 10 and 30% of its maximal value always remains. The inactivation time course could be fit by a sum of two exponentials. The fast component had a time constant of 200–300 msec, while the slower component had a time constant of 6–9 sec. The incompleteness of inactivation upon sustained depolarizing steps is also shown by experiments of steady-state inactivation. The results of these experiments, reported in Fig. 8*b* and *c* show that even for very depolarized conditioning prepulses of 5-sec duration, inactivation was not complete. Conditioning pulses more positive than 0 mV needed to be applied for more than 25 sec to fully inactivate the current.

The rate constant of recovery from inactivation was assessed by experiments (n = 3) of the type shown in Fig. 9*a*. The first pulse to +60 mV (duration 5 sec) was used to partially inactivate the I_{DRK}. The second pulse at the same voltage (+60 mV) was separated from the first by a variable interval at −70 mV, and used to assess the amount of current that had recovered from the preceding depolarization. In Fig. 9*b*, the fraction of current recovered, measured as described in the figure legend, is plotted as a function of the interval between pulses. I_{DRK} recovers to control levels within 2 sec after the inactivating prepulse. Similar experiments were carried out to

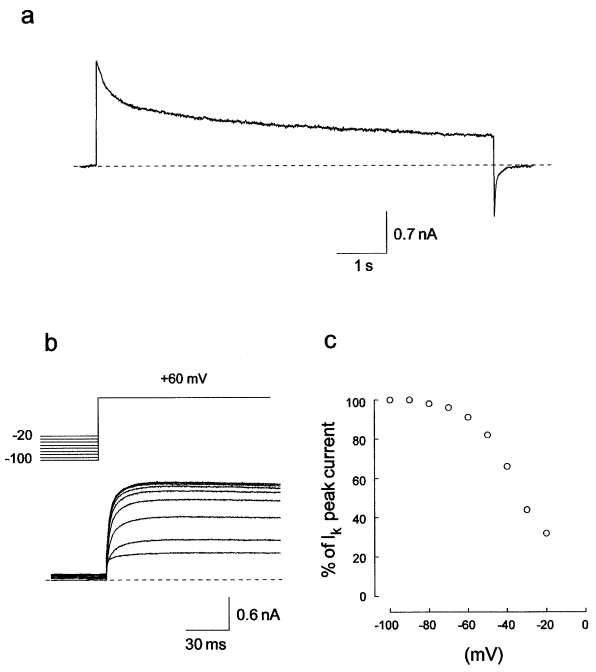

Fig. 8. Inactivation. (*a*) Inactivation time course during a sustained depolarizing pulse (10 sec) to +60 mV, from $V_H = -70$ mV. (*b*) I_{DRK} evoked by a fixed test pulse to +60 mV after 5 sec conditioning pulses to various potentials between −100 and −20 mV. (*c*) Current amplitudes normalized to the maximum current obtained at −100 mV were plotted against conditioning voltage.

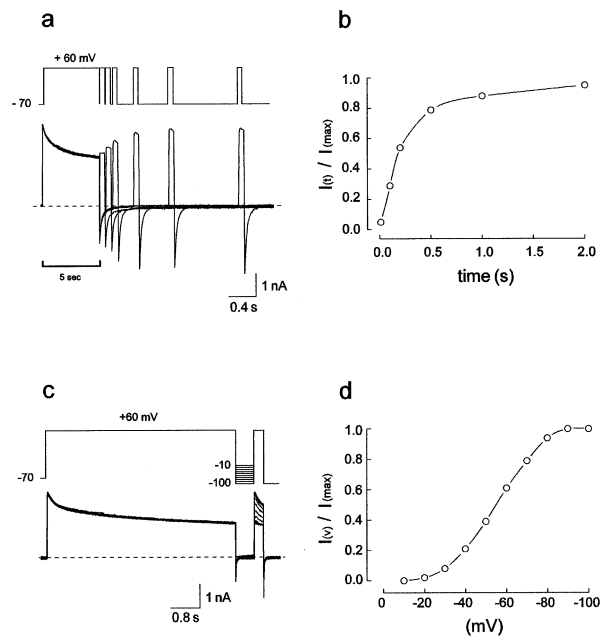

Fig. 9. Recovery from inactivation. (*a*) Time-dependent recovery from inactivation. A two-pulse protocol was used to measure the time course of recovery from inactivation. The first pulse from $V_H = -70$ to +60 mV for 5 sec activates and partially inactivates the I_{DRK}. The second pulse to same voltage was applied at progressively longer intervals from first pulse. Note different sampling rate for control and the remaining part of the figure *b.* Fraction of I_{DRK} expressed as I_{DRK} (second pulse)/I_{DRK} (first pulse), was plotted against interpulse interval, taking as zero the value of the current at the end of the first pulse. (*c*) Voltage dependence of recovery from inactivation. A two-pulse protocol was used for this measurement. The first pulse from $V_H = -70$ to +60 mV for 5 sec activates and partially inactivates the I_{DRK}. The second pulse to fixed voltage of +60 mV was delivered after a fixed interval of 500 msec during which the V_H was changed from −100 to −10 mV, in 10 mV intervals. (*d*) Fraction of I_{DRK} recovered expressed as above, was plotted as a function of interpulse V_H.

assess the dependence of recovery from voltage. Two depolarizing pulses were applied at a fixed interval of 500 msec at potentials ranging from −110 to −10 mV (Fig. 9*c*). In Fig. 9*d*, percentage of recovery is plotted as function of voltage.

Discussion

Channel Selectivity and Block

Following a selectivity pattern common to most DRK channels, the channel underlying the sustained outward current described here is readily permeant to K and Rb, and excludes Na and Li. The peculiar feature of this channel is its significant permeability to Cs ($P_{Cs}/P_K = 0.25$), which can sustain appreciable outward current. The only other qualitatively similar observation of a significant Cs permeability in DRK channels was reported in *Aplysia* neurons ($P_{Cs}/P_K = 0.18$; Reuter & Stevens, 1980), although other instances of measurable Cs permeation through DRK channels have been claimed (Cahalan et al., 1985; Hadley & Hume, 1990; Shapiro & DeCoursey, 1991; Block & Jones, 1999). Although Cs can permeate the DRK channels, when present in mixtures with K it can exert an appreciable block of the current, as shown by the anomalous mole-fraction effect it produces. Permeation and block displayed by Cs are not unreconcilable observations when occurring in a multi-site pore, as they may simply reflect the simultaneous presence of more than one ion in the pore. The finding that DRK channels show anomalous mole-fraction dependence of current when Cs gradually replaces K may indicate that K binds more tightly to the channel than Cs ($P_{Cs}/P_K = 0.25$), and is helped much more effectively in leaving the site by a second K ion in the pore that electrostatically destabilize it, than by the less tightly bound Cs ion. Several studies and the theory developed on this topic offer satisfactory explanations to such observations (Hille & Schwarz, 1978; Hess, Lansman & Tsien, 1984; Almers & McCleskey, 1984; Korn & Ikeda, 1995). The conclusion from this experiment is that like most DRK channels, the channel studied here

has a long pore with more than one ion simultaneously in the channel moving in single file.

The other finding of this study is the block of I_{DRK} by Verapamil at micromolar concentrations. Several papers have reported a block of noninactivating or slowly inactivating K currents by this drug (Kostyuk, Krishtal & Doroshenko, 1975; Galietta et al., 1991; Pancrazio et al., 1991; Rampe et al., 1993; DeCoursey, 1995). We found, in accordance with other studies, that Verapamil exerts its block in a state-dependent manner (*cf.* Armstrong, 1971; French & Shoukimas, 1981; Snyders et al., 1991; DeCoursey, 1995). This is shown by the good fit of the time course of Verapamil-blocked I_{DRK} (*cf.* Fig. 4*a*) that could be obtained with the equation derived from the kinetic scheme of open-channel block (for details *cf.* Materials and Methods and legend to Fig. 4), and by the frequency-dependent effect that Verapamil exerts on I_{DRK} (Fig. 4*c*). Affinity of Verapamil for the blocking site, and molecularity of the blocking reaction were determined from the dose-response plot (Fig. 4*b*). Data were fit by a single-site absorption isotherm which indicates a first-order kinetics of block, and gave a K_D of 3.9 μM. Note that this value is in good agreement with the K_D value that can be derived from the kinetic constants of block, *k* and *l*, obtained by fitting the decay time course of I_{DRK} in the presence of Verapamil (*cf.* legend to Fig. 4).

KINETICS

Activation and Inactivation

Although K channels are made of four identical subunits, each carrying a putative voltage sensor, the activation of the I_{DRK} could not be described by a fourth power of a first-order kinetics (*cf.* Results). Following strong hyperpolarizing pulses, Cole and Moore (1960) found that the description of I_{DRK} activation needed the kinetic constants to be raised to powers much higher than four. Similar difficulties induced several other authors (Gilly & Armstrong, 1982; White & Bezanilla, 1985; Spires & Begenisich, 1989) to abandon classical descriptions of I_{DRK} activation (i.e., abandon the constraint of Hodgkin and Huxley (1952) formalism with respect to the number of closed states—in modern thinking—the number of voltage sensors). Keynes, Kimura & Greeff (1988) modified the classical fourth power equation by incorporating a second larger time constant to accommodate the slow upward creep following the initial inflection of I_{DRK} in the squid giant axon. More recently Koumi et al. (1994) found that the I_{DRK} from pig hepatocytes was better described by a linear kinetic model with two closed and one open state. In both cases, the double component resulted from a strictly single population of channels. As anticipated in the Results section, although we chose to provide the activation time constants of single-exponential fit of only the fast upward inflection of the current, we most often found that the addition of a second component would better describe the full time course of the current.

Also the inactivation of I_{DRK} during maintained depolarized pulses occurred with two distinct time constants of *ca.* 200–300 msec, and 6–9 sec, respectively. The double component of activation and inactivation kinetics could suggest the presence of two kinetically distinct populations of DRK channels. Two distinct DRK channels with different (7 and 50 pS) conductance have indeed been identified in mammalian sensory neurons (Kasai et al., 1986). On the other hand, we have seen that a double component of activation can result from a single population of channels (*cf.* Keynes et al., 1988; Koumi et al., 1994). Similarly, a double component of inactivation has been shown to result from two distinct inactivation mechanisms present on the same channel (Choi, Aldrich & Yellen, 1991): A fast inactivation, depictable by the ''ball and chain'' mechanism, where the ball is played by the intracellular NH_2-terminal, and a slow inactivation supposedly involving the S6 alpha-helical segment of the channel. Also in our case, the double component of activation and inactivation is more likely the result of a single-channel population, as indicated by the good fits of the activation data by a single Boltzmann (Fig. 7), and of the dose-response curve by a single Hill isotherm (Fig. 3). (With respect to the Hill plot, the possibility that the second channel population is not sensitive to Verapamil is not tenable since high drug concentration completely abolishes the current.)

Deactivation

Deactivation time course, studied from tail currents, followed a mono-exponential decay whose time constant was a function of voltage. Time constants ranging from *ca.* 25 msec at −90 mV to *ca.* 95 msec at −40 mV (Fig. 6*c*) indicate a slow deactivation kinetics which is several times slower than the deactivation time constant of most I_{DRK}. Slow deactivation kinetics have in certain cases been associated with hindrance effects of permeant or impermeant ions on the channel gate (the ''foot in the door'' effect; *cf.* Swenson & Armstrong, 1981; Matteson & Swenson, 1986). This interpretation however would not account for our observations since deactivation rates were not seen to change with different perfusing ions or with their concentration, as expected if ions would prevent (or impair) the channel from closing. The possibility that the slow decay could result from the activation of a Ca-activated Cl current (we showed already that a Ca-activated K current can be excluded) could likewise be ruled out since replacement of Cl ions with impermeant glutamate did not change the deactivation rate of the

current. It is more likely therefore that in this preparation the slow off-rate of the current reflects an intrinsic gating property of the DRK channels.

Another peculiar feature of I_{DRK} is that activation and deactivation time constants, plotted as a function of voltage (Fig. 6*c*), do not converge to a maximum near the activation $V_{1/2}$, as observed in most DRK channels. This suggests that channel activation (i.e., the transition between the last closed state and the open state) and deactivation kinetics cannot be approximated by a first order transition between those two states. In other words, the channels would deactivate (close) via a pathway different from the reverse sequence of activation. The DRK channels would thus activate by a linear sequence of transitions through a series of closed states (to account for the initial delay) to the open state, but they would deactivate following a different pathway connecting the open state and closed states, possibly including an additional nonconducting state through which the channel must pass before closing, upon repolarization.

We thank Drs. David Adams and Sandy Harper for their comments on the manuscript. This work was supported by grant 92.689.CT04/115.21260 from Italian Consiglio Nazionale Ricerche.

References

Adelman, W.J., French, R.J., Jr. 1978. Blocking of the squid axon potassium channel by external caesium ions. *J. Physiol.* **276:**13–25

Almers, W., McCleskey, E.W. 1984. Non-selective conductance in calcium channels of frog muscle: calcium selectivity in a single-file pore. *J. Physiol.* **353:**585–608

Almers, W., McCleskey, E.W., Palade, P.T. 1984. A non-selective cation conductance in frog muscle membrane blocked by micromolar external calcium ions. *J. Physiol.* **353:**565–583

Armstrong, C.M. 1971. Interaction of tetraethylammonium ion derivates with the potassium channels of giant axons. *J. Gen. Physiol.* **58:**413–437

Barde, Y.A., Edgard, D., Thoenen, H. 1980. Sensory neurons in culture: changing requirements for survival factors during embryonic development. *Proc. Natl. Acad. Sci. USA* **77:**1199–1203

Belluzzi, O., Sacchi, O., Wanke, E. 1985. A fast transient outward current in the rat sympathetic neurone studied under voltage-clamp conditions. *J. Physiol.* **358:**91–108

Bezanilla, F., Armstrong, C.M. 1972. Negative conductance caused by entry of sodium and cesium ions into the potassium channels of squid axons. *J. Gen. Physiol.* **70:**588–608

Binstock, L., Lecar, H. 1969. Ammonium ion currents in the squid giant axon. *J. Gen. Physiol.* **53:**342–361

Block, B.M., Jones, S.W. 1996. Ion permeation and block of M-type and delayed rectifier potassium channels. *J. Gen. Physiol.* **107:**473–488

Byerly, L., Hagiwara, S. 1982. Calcium currents in internally perfused nerve cell bodies of Limnea stagnalis. *J. Physiol* **322:**503–528

Cahalan, M.D., Chandy, K.C., DeCoursey, T.E., Gupta, S. 1985. A voltage-gated potassium channel in human T lymphocytes. *J. Physiol.* **358:**197–237

Catterall, W.A. 1988. Structure and function of voltage-sensitive ion channels. *Science* **242:**50–61

Choi, K.L., Aldrich, R.W., Yellen, G. 1991. Tetraethylammonium blockade distinguishes two inactivation mechanism in voltage-activated K channels. *Proc. Natl. Acad. Sci. USA* **88:**5092–5095

Cole, K.S., Moore, J.W. 1960. Ionic current measurements in the squid giant axon membrane. *J. Gen. Physiol.* **44:**123–167

Colquhoun, D., Hawkes, A.G. 1977. Relaxation and fluctuations of membrane currents that flow through drug-operated ion channels. *Proc. R. Soc. Lond.* **199:**231–262

Connor, J.A., Stevens, C.F. 1971. Voltage clamp studies of a transient outward membrane current in gastropod neural somata. *J. Physiol.* **213:**21–30

DeCoursey, T.E. 1995. Mechanism of K^+ channel block by Verapamil and related compounds in rat alveolar epithelial cells. *J. Gen. Physiol.* **106:**745–779

Ehrenstein, G., Gilbert, D.L. 1966. Slow changes of potassium permeability in the squid giant axon. *Biophys. J.* **6:**553–566

Fenwick, E.M., Marty, A., Neher, E. 1982. Sodium and calcium channels in bovine chromaffin cells. *J. Physiol.* **331:**599–635

French, R.J., Shouikimas, J.J. 1981. Blockage of squid axon potassium conductance by internal tetra-n-alkylammonium ions various sizes. *Biophys. J.* **34:**271–291

French, R.J., Wells, J.B. 1977. Sodium ions as blocking agents and charge carriers in the potassium channel of the squid giant axon. *J. Gen. Physiol.* **70:**707–724

Fukushima, Y., Hagiwara, S. 1985. Current carried by monovalent cations through calcium channels in mouse neoplastic B lymphocytes. *J. Physiol.* **358:**255–284

Galietta, L.J., Rasola, V.A., Barone, V., Gruenert, D.C., Romeo, G. 1991. A forskolin and Verapamil-induced blockade of voltage-activated K^+ current in small-cell lung cancer cells. *Biochem. Biophys. Res. Commun.* **179:**1155–1160

Gilly, W.F., Armstrong, C.M. 1982. Divalent cations and the activation kinetics of potassium channels in Squid giant axons. *J. Gen. Physiol.* **79:**965–996

Hadley, R.W., Hume, J.R. 1990. Permeation of Cs, Na, NH_4, and Rb through the delayed rectifier in guinea-pig ventricular myocytes. *Biophys. J.* **57:**141*a.* (*Abstr.*)

Hamill, O.P., Marty, A., Neher, E., Sakmann, B., Sigworth, F.J. 1981. Improved patch-clamp techniques for high-resolution current recording from cells and cell-free membrane patches. *Pfluegers Arch.* **391:**85–100

Hermann, A., Gormann, A.L.F. 1981. Effect of 4-aminopyridine on potassium currents in a molluscan neuron. *J. Gen. Physiol.* **78:**63–86

Hess, P., Lansman, J.B., Tsien, R.W. 1984. Different modes of Ca channel gating behaviour favoured by dihydropyridine Ca agonists and antagonists. *Nature* **311:**538–544

Hille, B. 1973. Potassium channels in myelinated nerve. Selective permeability to small cations. *J. Gen. Physiol.* **61:**669–686

Hille, B., Schwarz, W. 1978. Potassium channels as multi-ion single-file pores. *J. Gen. Physiol.* **72:**409–442

Hodgkin, A.L., Huxley, A.F. 1952. A quantitative description of membrane current and its application to conduction and excitation in nerve. *J. Physiol.* **116:**500–544

Kasai, H., Kameyama, M., Yamaguchi, K., Fukuda, J. 1986. Single transient K channels in mammalian sensory neurons. *Biophys. J.* **49:**1243–1247

Keynes, R.D., Kimura, J.E., Greeff, N.G. 1988. Kinetics of activation of the potassium conductance in the squid giant axon. *Proc. R. Soc. Lond.* **B232:**315–351

Korn, S.J., Ikeda, S.R. 1995. Permeation selectivity by competition in a delayed rectifier potassium channel. *Science* **269:**410–412

Kostyuk, P.G., Krishtal, O.A. 1977. Effects of calcium and calcium-chelating agents on the inward and outward current in the membrane of mollusc neurones. *J. Physiol.* **270:**659–580

Kostyuk, P.G., Krishtal, O.A., Doroshenko, P.A. 1975. Outward currents in isolated snail neurones. III. Effects of Verapamil. *Comp. Biochem. Physiol.* **51C:**269–274

Kostyuk, P.G., Veselovsky, N.S., Fedulova, S.A., Tsyndrenko, A.Y. 1981. Ionic currents in the somatic membrane of rat dorsal root ganglion neurons-III. Potassium currents. *Neuroscience* **6:**2439–2444

Koumi, S., Sato, R., Horikawa, T., Aramaki, T., Okumura, H. 1994. Characterization of the calcium-sensitive voltage-gated delayed rectifier potassium channel in isolated Guinea pig hepatocytes. *J. Gen. Physiol.* **104:**147–171

Lee, K.S., Tsien, R.W. 1982. Reversal of current through calcium channels in dialysed single heart cells. *Nature* **297:**498–501

MacKinnon, R. 1991. Determination of the subunit stoichiometry of a voltage-activated potassium channel. *Nature* **350:**232–235

Matteson, D.R., Swenson, R.P., Jr. 1986. External monovalent cations that impede the closing of K channels. *J. Gen. Physiol.* **87:**795–816

Meves, H., Pichon, Y. 1977. The effect of internal and external 4-aminopyridine on the potassium currents in intracellularly perfused squid giant axons. *J. Physiol.* **268:**511–532

Neher, E. 1971. Two fast transient current components during voltage clamp on snail neurons. *J. Gen. Physiol.* **58:**36–53

Nowycky, M.C. 1992. Voltage-gated ion channels in dorsal root ganglion neurons. *In:* Sensory Neurons, S.A. Scott, editor. Oxford University Press

Pancrazio, J.J., Viglione, M.P., Kleiman, R.J., Kim, Y.I. 1991. Verapamil-induced blockade of voltage-activated K current in small-cell lung cancer cells. *J. Pharm. Exp. Ther.* **257:**184–189

Pelhate, M., Pichon, Y. 1974. Selective inhibition of potassium current in the giant axon of the cockroach. *J. Physiol.* **242:**90–91P

Rampe, D., Wible, B., Fedida, D., Dage, R.C., Brown, A.M. 1993. Verapamil blocks a rapidly activating delayed rectifier K channel cloned from human heart. *Mol. Pharmacol.* **44:**642–648

Reuter, H., Sholz, H. 1977. A study of the ion selectivity and the kinetic properties of the calcium dependent slow inward current in mammalian cardiac muscle. *J. Physiol.* **264:**17–47

Reuter, H., Stevens, C.F. 1980. Ion conductance and ion selectivity of potassium channels in snail neurones. *J. Membrane Biol.* **57:**103–118

Schauf, C.L., Colton, C.A., Colton, J.S., Davis, F.A. 1976. Aminopyridines and sparteine as inhibitors of membrane potassium conductance: effects on Myxicola giant axon and the lobster neuromuscular junction. *J. Pharm. Exp. Ther.* **197:**414–425

Schwarz, J.R., Wogel, W. 1971. Potassium inactivation in single myelinated nerve fibres of *Xenopus laevis*. *Pfluegers Arch.* **330:**61–73

Shapiro, M.S., DeCoursey, T.E. 1991. Selectivity and gating of the type L Potassium channel in mouse lymphocytes. *J. Gen. Physiol.* **97:**1227–1250

Snyders, D.J., Knoth, K.M., Roberds, S.L., Tamkun, M.M. 1991. Time-, voltage-, and state-dependent block by quinidine of a cloned human cardiac potassium channel. *Mol. Pharmacol.* **41:**322–330

Spires, S., Begenisich, T. 1989. Pharmacological and kinetic analysis of K channel gating currents. *J. Gen. Physiol.* **93:**263–283

Swenson, R.P., Armstrong, C.M. 1981. K channels close more slowly in the presence of external K and Rb. *Nature* **291:**427–429

Ulbricht, W., Wagoner, H.H. 1976. Block of potassium channels of the nodal membrane by 4-aminopyridine and its partial removal on depolarization. *Pfluegers Arch.* **367:**77–87

White, M.M., Bezanilla, F. 1985. Activation of squid axon K channels: ionic and gating current studies. *J. Gen. Physiol.* **85:**539–554

Yeh, J.Z., Oxford, G.S., Wu, C.H., Narahashi, T. 1976. Dynamics of aminopyridine block of potassium channels in squid axon membrane. *J. Gen. Physiol.* **68:**519–535